Electromagnetic Field Emission From Gas-to-Air Bushing in a GIS During Switching Operations

M. Mohana Rao, M. Joy Thomas, and B. P. Singh

***Abstract*—Very fast transient overvoltages (VFTOs) and the associated very fast transient currents (VFTCs) generated during switching operations in a gas-insulated substation (GIS) radiate electromagnetic (EM) fields, which in turn can leak into the external environment through apertures like SF_6 gas-to-air bushing. Therefore, it becomes necessary to characterize and quantify the EM fields when sensitive control devices are used for the operation of such substations. Keeping this in view, a numerical model using a finite-difference time-domain (FDTD) technique was developed to compute the transient field emission from a 245-kV-rated gas-to-air bushing. Shielding effectiveness (SE) of the bushing for these transient fields was evaluated using a derivative Gaussian current excitation of the high-tension (HT) conductor. The variation in EM field levels along the axis of bushing at various radial distances for different frequencies of the transient current were analyzed. The enhancement of the field levels due to the presence of a metallic structure on the ground plane, which simulates the control cubicle or the grounded enclosures of the GIS, were studied. Finally, the emission levels from different bushing models were calculated for the VFTC generated during a switching event, and the dominant frequencies were identified.**

***Index Terms*—Electromagnetic interference (EMI), finite-difference time-domain (FDTD), gas-insulated substation (GIS), switching, very fast transient currents (VFTCs), very fast transient overvoltages (VFTOs).**

I. Introduction

In a gas-insulated substation (GIS), very fast transient overvoltages (VFTOs) are generated due to switching operations. These transient overvoltages and the associated very fast transient currents (VFTCs) could have a rise time of the order of 4 ns and above [1]. The peak magnitude of the transient current may be about a few kiloamperes depending on the location of the switch operated, the substation layout, and the observation point. These transient voltages/currents radiate electromagnetic (EM) fields during their propagation along the coaxial high-voltage (HV) bus of the GIS, as the associated frequencies are in the range of a few megahertz to about a few hundreds of megahertz. The transient EM fields, in turn, leak into the external environment through apertures like SF_6 gas-to-air bushing, gas-to-cable termination, nonmetallic viewing ports, insulated flanges, etc., and couple to the control equipment/data cables present within the GIS. This coupling produces transient current/voltage on the shield of the control cable. Depending on the transfer impedance between the shield and the central conductor of the cable, transient voltage appears at the terminals of the control cable. Pigtail coupling can also take place between the shield pigtail and the central conductor of the cable [2]. Each switching operation produces multiple transient EM fields, and the number of transients may vary with the rated voltage of the substation, type/speed of the switch, and the electrical characteristics of the HV bus being operated [3], [4].

The numerical/experimental quantification of the emission levels from the bushing during switching events has been found to be important for the electromagnetic compatibility (EMC) design of the control/protection equipment operating in such a harsh electromagnetic interference (EMI) environment, and thereby, for a reliable operation of the systems [5]. For characterizing the transient EMI in a GIS, it is essential to predict the EM fields emitting from the gas-to-air bushing due to the VFTC generated during switching events. The transient EMI has to be fully characterized in terms of the time-domain waveforms and their frequency spectra for the highest expected levels both at/near the GIS primary equipment (i.e., HV equipment) and within the secondary equipments (control cubicle, control cables, embedded sensors, etc.). These EMI levels may then be compared with the susceptibility levels of the control equipment for temporary upset or permanent damage. Several authors [1]–[4] have carried out measurements to ascertain the levels of emission during switching operations. These measurements have been proven to be expensive, and the computational techniques-based quantification of the transient EMI is gaining practical importance in recent years [2], [4].

In this paper, the EM field emission levels from the gas-to-air bushing during a switching operation have been computed. The validity of the computational model is confirmed by calculating the EM fields for a sinusoidal current excitation of the HT conductor and compared with the field levels, estimated by using the magnetic vector potential approach. The shielding effectiveness (SE) of the bushing for the EM fields is evaluated using a derivative Gaussian current and a sinusoidal current source. The effect of conductivity of the ground and presence of the metallic/insulated structures on the field pattern is analyzed in the study. Finally, the variation in emission levels and their frequency content from various models of the bushing due to the VFTC has been reported.

II. VFTC

The peak magnitude and the frequency content of VFTCs generated during switching operations are highly dependent on the GIS configuration as well as the observation point. The transient current magnitude at the GIS-bushing junction in the

Manuscript received August 5, 2005; revised October 4, 2006.

M. M. Rao and B. P. Singh are with Corporate R&D, Bharat Heavy Electricals Limited, 500093 Hyderabad, India (e-mail: mmrao@bhelrnd.co.in; bpsingh@bhelrnd.co.in).

M. J. Thomas is with the Department of High Voltage Engineering, Indian Institute of Science, 560012 Bangalore, India (e-mail: thoma@hve.iisc.ernet.in).

Digital Object Identifier 10.1109/TEMC.2007.893334

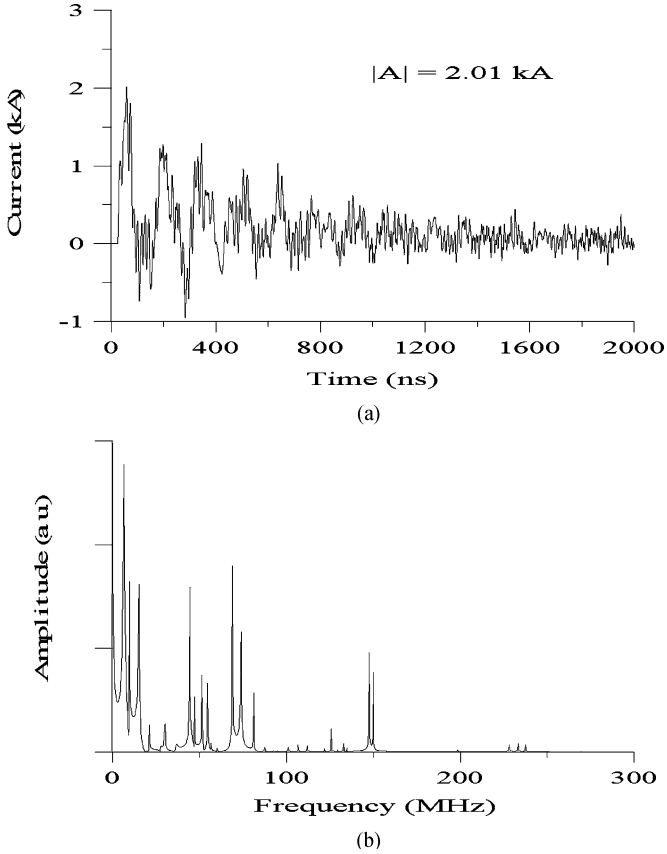

Fig. 1. VFTC waveform and its frequency spectrum at GIS-bushing junction.

245-kV GIS is about 1 kA, and the frequency components of the transient currents are generally well below 74.5 MHz [6]. However, in special situations like switching of a smaller length of the bus section, with the switch located at a distance of few meters from the bushing, peak current magnitude of about 2 kA and frequency content up to 150 MHz are also possible (see Fig. 1). The VFTC waveform has been calculated for the closing operation of the disconnector switch (DS) in a 245-kV GIS by considering the earlier conditions. The highest magnitude of the transient current occurs near the DS, and it decreases with the increasing distance from the switch [6]. The frequency spectrum of the VFTC waveform has been calculated using the fast Fourier transform (FFT) technique.

III. FDTD Technique

In FDTD technique, Maxwell's curl equations are discretized both in time and space using central difference approximation [7]. The computational region, i.e., the solution region, is divided into cells with the corresponding electric and magnetic fields located on the edges and the faces, respectively. It is assumed that all the fields in the entire solution region are zero at the beginning of the computation. Suitable boundary conditions on the artificial boundary have been imposed to simulate the extension of the solution region to infinity [8]. For modeling the slots and thin metallic walls of bushing, the contour integral approach has been adopted [9].

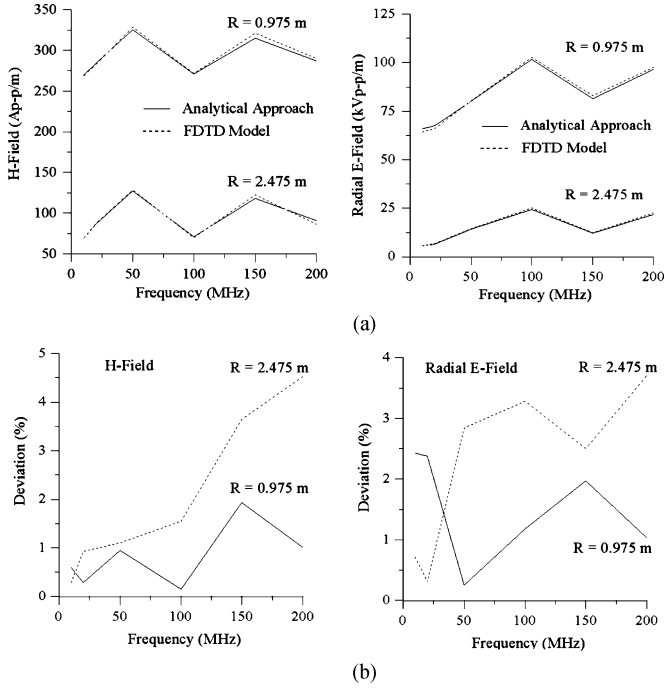

Fig. 2. Computation of EM fields for analytical and FDTD models.

IV. Validation of the Model

The EM field levels due to the transient current excitation of the HT conductor have been calculated by using the magnetic vector potential approach (analytical model) as well as the FDTD model developed in this paper. Here, the HT conductor of the bushing is only considered for the computation. A variable frequency sinusoidal current source of amplitude 1 kA for total time duration of 2 μs is used as an excitation. The above computation is required to validate the model developed in the study. The azimuthal magnetic field (H_ϕ), radial E-field (E_r), and axial E-field (E_z) have been calculated at different radial distances (R) from the current source and axially at the middle of the HT conductor using the analytical approach and the FDTD model. Fig. 2(a) shows the EM field levels calculated using the above two techniques for the entire frequency range of the VFTC. The field levels calculated using the FDTD model deviate marginally from the values obtained using the analytical model. The percentage deviation is shown in Fig. 2(b). It is further noticed that the highest EM field level need not occur at middle of the HT conductor for all the frequencies of the transient current [10]. The field levels calculated using the FDTD model deviate considerably from the analytical model when the observation point approaches the boundary of the computational domain as its size is less than $\lambda/6$ of the corresponding frequency of the transient fields [7], [8]. In view of these, the computational domain dimensions have been chosen in such a way that the EM fields can be calculated even for low-frequency currents with reasonable accuracy.

V. Gas-to-Air Bushing Model

Fig. 3 shows the schematic diagram of a 245-kV-rated gas-to-air bushing along with a portion of the gas-insulated bus

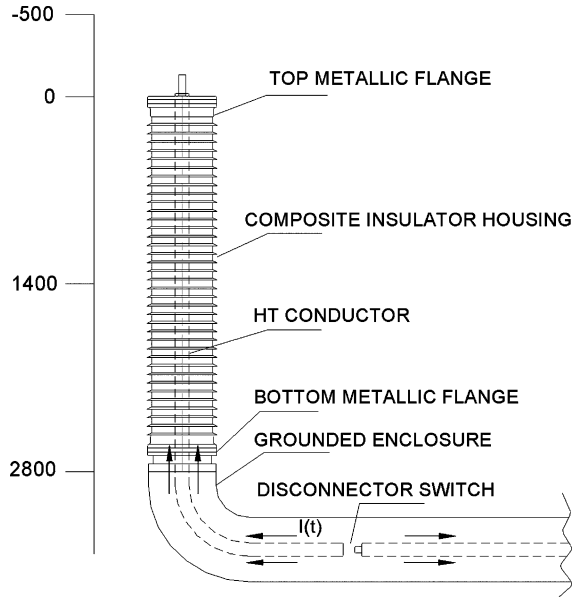

Fig. 3. Schematic diagram of the 245-kV gas-to-air bushing under study (all dimensions shown are in millimeters).

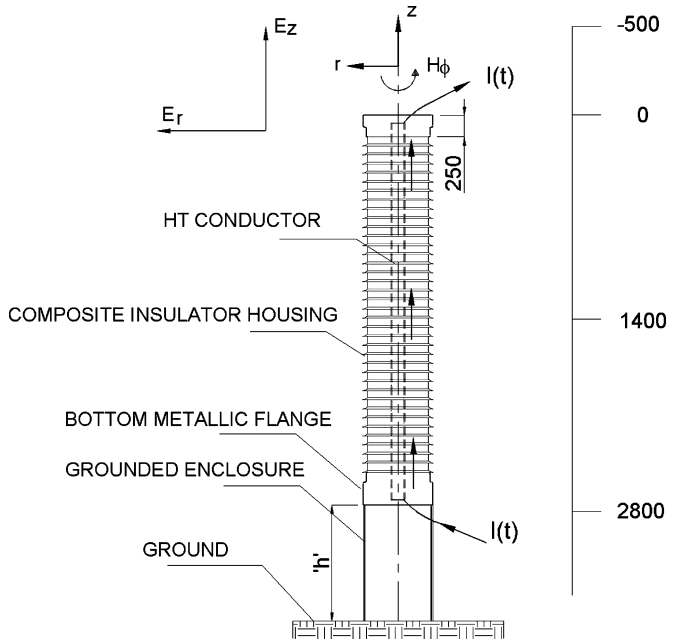

Fig. 4. Equivalent model of the gas-to-air bushing installation.

section of the GIS. The transient fields generated internally to the bushing due to the transient currents, leak into the external environment through the composite insulator housing ($\varepsilon_r = 3$). The thickness of the composite insulator housing is considered to be 50 mm. The outer diameter of the HT conductor and the inner diameter of the grounded enclosure are 100 and 400 mm, respectively. Fig. 4 shows the equivalent model of the bushing installation considered for the study. The transient current $I(t)$, is assumed to propagate from bottom to top of the HT conductor. Even though the HT connection from the bushing continues, the contribution of EM fields due to the current propagating along the HT conductor is only computed. This is for the purpose of calculating the SE of the bushing for the EM fields.

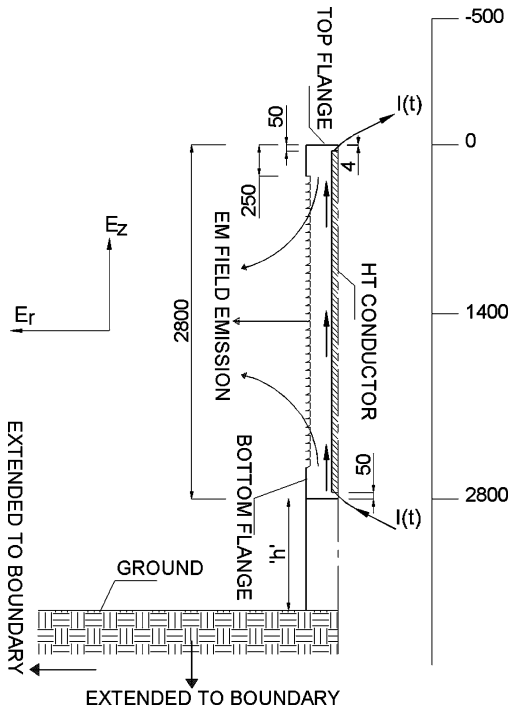

Fig. 5. FDTD model of the gas-to-air bushing installation.

TABLE I
TRANSIENT EM FIELDS FOR VARIOUS FREQUENCIES OF TRANSIENT CURRENT

(a). 5 MHz

No. of cells (cell size)	H_ϕ-field ($A_{p\text{-}p}$/m)		E_r-field ($kV_{p\text{-}p}$/m)	
	R=0.975m	R=2.475m	R=0.975m	R=2.475m
200x100 (50 mm)	249.2	55.2	58.2	5.35
400x200 (50 mm)	250.0	57.6	58.1	5.13
600x300 (50 mm)	250.0	57.8	57.9	5.06

(b). 200 MHz

No. of cells (cell size)	H_ϕ-field ($A_{p\text{-}p}$/m)		E_r-field ($kV_{p\text{-}p}$/m)	
	R=0.975m	R=2.475m	R=0.975m	R=2.475m
400x200 (50 mm)	280.0	96.0	101.0	19.6
800x400 (25 mm)	284.5	102.5	102.3	20.3
800x400(12.5mm)	286.4	100.4	98.2	19.9

Fig. 5 shows the numerical model of the bushing installation above the ground plane in a GIS. To optimize the computational domain dimensions with the appropriate cell size, EM fields have been computed using sinusoidal current source of frequencies 5 and 200 MHz, for different cell sizes/domain dimensions (see Table I). The EM field emission levels from the bushing are calculated by optimizing the cell size to 50 mm $\times$ 50 mm with the number of cells limited to 400 $\times$ 200 in axial and radial directions, respectively. The peak magnitude of the EM fields is observed to be a function of the length of the current source, frequency of the current, and location of the observation point [11].

VI. SE OF THE GAS-TO-AIR BUSHING

In order to understand the effect of various parameters on the EM field emission levels, it is necessary to calculate the SE of the bushing installation for these EM fields. For this purpose, the derivative Gaussian current as well as the sinusoidal current

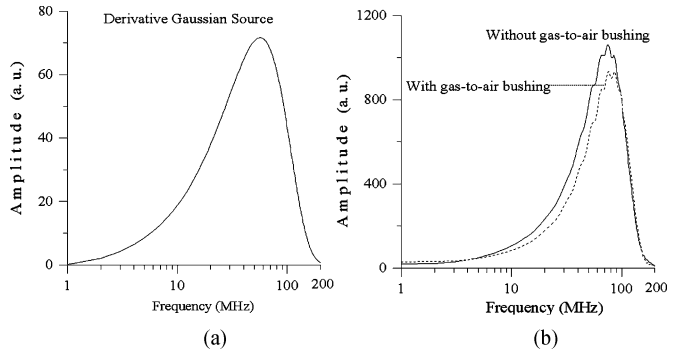

Fig. 6. Derivative Gaussian current excitation of the bushing. (a) Current source. (b) Radial E-field emission.

excitation of the HT conductor has been considered, in this paper.

A. Derivative Gaussian Current Excitation of the Bushing

The frequency spectrum of the Gaussian pulse contains a spectrum of energy, which is fairly flat up to a given frequency and then drops off rapidly. Since the spectrum has a dc component, it may result in a divergent or inaccurate solution to the computational model defined for a particular frequency range, and hence, is not suitable for the present application. When a Gaussian pulse is differentiated, the dc component of the pulse is removed, and it can be applied to the model proposed in this paper. The parameters of this derivative Gaussian source are selected in such a way that it associates with the entire frequency range of the VFTC. Fig. 6 shows the radial E-field at a distance of 2 m (located at middle of the HT conductor) due to the derivative Gaussian current excitation. The SE of the bushing for EM fields is observed to be dependent on the location of the observation point. Thus, the SE of the bushing for the EM fields could be defined as follows:

$$\mathrm{SE}_E\,(\mathrm{dB}) = -20\,\log 10\,(E_{1m}/E_{0m}) \tag{1}$$

$$\mathrm{SE}_H\,(\mathrm{dB}) = -20\,\log 10\,(H_{1m}/H_{0m}) \tag{2}$$

where E_{1m} and E_{0m} are the highest E-fields at a particular radial distance (by considering the entire axial distance) with and without the gas-to-air bushing, respectively. H_{1m} and H_{0m} have a similar H-field connotation. Fig. 7 shows the SE of the bushing for the transient EM fields. From this figure, the following observations have been made.

1) SE for H-fields decreases with the increase of frequency, and the bushing does not offer any attenuation for these fields beyond 55 MHz. The SE pattern for H-fields and axial E-fields is almost similar beyond the transition frequency, i.e., 28 MHz. The SE for radial E-fields also decreases with the increase of frequency, and the bushing does not offer any attenuation to the radial E-fields beyond 80 MHz.
2) The SE of the bushing for E-fields and H-fields is very low (for H-fields at 20 MHz, SE is of the order of 0.7 dB).

In order to validate the earlier results, SE was calculated at a radial distance of 4 m from the bushing, and it was observed

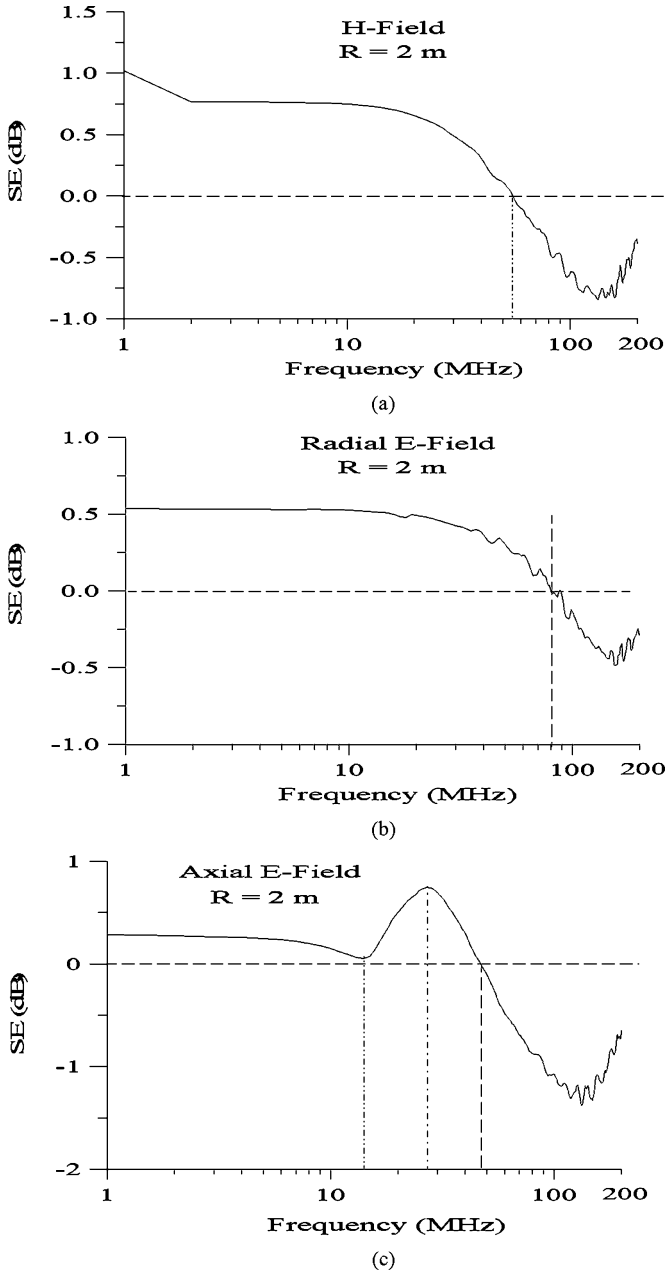

Fig. 7. Shielding effectiveness of the bushing for the transient EM fields.

that the SE for the EM fields does not change significantly with radial distance (at 20 MHz, SE is of the order of 0.78 dB). Also, at a radial distance of 4 m, beyond 52 MHz, bushing does not offer any attenuation to the H-fields and axial E-fields. The SE pattern for H-fields and axial E-fields is again similar, beyond the transition frequency, i.e., 16 MHz. This frequency depends on the radial distance from the bushing and the dimensions of the bushing/HT conductor.

B. Sinusoidal Current Excitation of the Bushing

In order to quantify the emission levels from the bushing, it is important to know its behavior for continuous time-varying fields. As such, EM fields have been calculated for sinusoidal current excitation of the HT conductor. For the bushing model

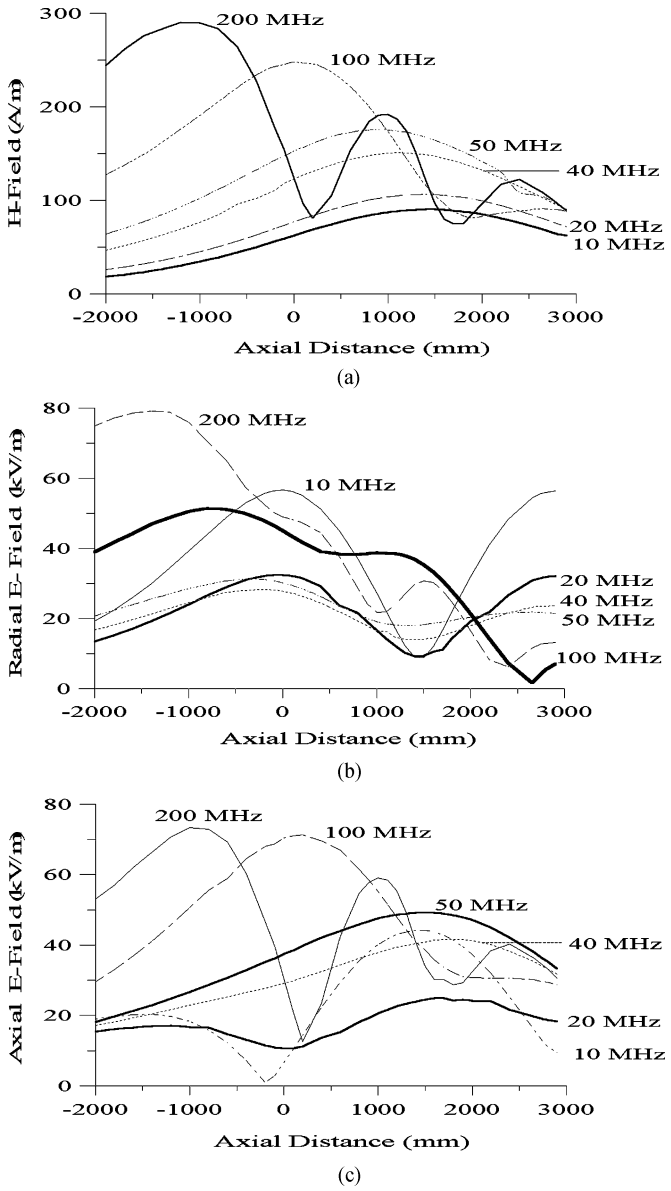

Fig. 8. Variation of the transient EM fields at a radial distance of 2 m.

with a very low conductivity ground (10^{-6} mho/m), the EM field levels decrease with the increase of radial distance from the HT conductor, for the entire frequency range of the VFTC. However, at a particular radial distance, these field levels change with the observation point in the axial direction. Fig. 8 shows the variation of the emission levels (peak-to-peak magnitude of EM field waveforms) along the axis of bushing with frequency, at a distance of 2 m. As expected, the location of highest magnitude/amplitude of the EM fields in the axial direction changes with the frequency of the current source. For the transient current of frequency below the cut-off frequency (depending on the length of the current source, i.e., close to $\lambda/2$), the highest magnitude of the H-field occurs near the middle of the bushing. Beyond this frequency, there is a possibility of oscillatory variation for the H-field level, from the top to bottom flange with considerable attenuation. The highest H-field level at a particular distance increases with increase of frequency of the current

TABLE II
TRANSIENT EM FIELD EMISSION LEVELS FROM THE BUSHING

f (MHz)	H-field ($A_{p\text{-}p}$/m)		SE_H (dB)	E_r-field ($kV_{p\text{-}p}$/m)		SE_E (dB)
	C1	C2		C1	C2	
5	92.3	84.6	0.757	116.2	109.5	0.516
10	98.4	90.5	0.727	60.0	56.6	0.507
20	114.4	106.3	0.638	34.3	32.5	0.468
40	153.5	150.7	0.160	29.3	28.2	0.332
50	177.5	175.6	0.093	32.2	31.2	0.274
100	228.7	248.0	-	50.0	51.4	-
150	260.1	285.1	-	65.1	69.0	-
200	277.8	290.1	-	76.5	79.2	-

C1 – HT conductor only ; C2– with gas-to-air bushing

irrespective of the field region (i.e., near-field or far-field). Similarly, below the cut-off frequency, the highest amplitude of the radial E-field appears at/near the top/bottom flanges and the lowest amplitude occurs at middle of the bushing. This may be due to the almost equal and opposite contribution of radial E-field from either end of the current source. At higher frequencies, the location of highest magnitude starts to move away from the top flange (i.e., above the bushing depending on radial distance). Further, the highest radial E-field level increases with the increase of frequency beyond the transition frequency. The variation of radial E-field along the axis of bushing is found to be highly sensitive to the field region unlike to that for the H-field. The axial E-field variation at a radial distance of 2 m is almost similar to the H-field except for the frequencies of 10 and 20 MHz. This may be due to the observation point being in near-field region for these frequencies of the current.

The highest EM field levels at a radial distance of 2 m from the bushing, for the transient current of different frequencies, are listed in Table II. The results again confirmed that the SE of the bushing for EM fields is very low. SE for H-fields and radial E-fields decreases with the increase of frequency up to 50 MHz (close to the cut-off frequency). Above this frequency, there is a slight increase in the highest EM field levels, due to the presence of the composite insulator housing as well as the top/bottom flanges. To understand the effect of location of the observation point on the EM field pattern, E and H field levels have been computed at a radial distance of 4 m. At this radial distance also, the highest H-field magnitude increases with increasing frequency of the current. The axial E-field variation at a radial distance of 4 m is almost similar to the H-field pattern except for a current source of 10-MHz frequency. The same phenomenon has been observed even for the derivative Gaussian current excitation of the bushing.

VII. ENHANCEMENT OF THE TRANSIENT EM FIELDS

The enhancement of the EM field levels has been studied for two configurations that are quite often possible in a GIS. One is due to a metallic ground and the other is due to a metallic structure (e.g., a control panel) on the ground. To calculate the enhancement due to a metallic ground, EM field levels have been computed along the axis of the bushing at a radial distance of 2 m, with normal as well as metallic ground. The highest field levels are calculated at each frequency using derivative Gaussian current excitation, and it is found that the enhancement is well

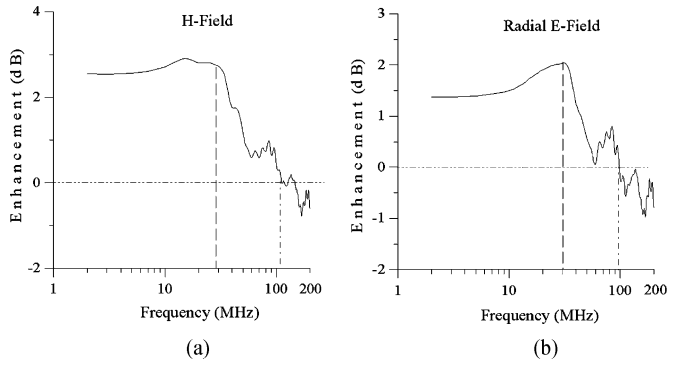

Fig. 9. Enhancement of the EM field emission levels from the bushing with a metallic sheet on the ground plane. (a) H-field. (b) E_r-field.

below 3 dB (Fig. 9). The results indicated that, beyond the transition frequency, there is a possibility of decrease in the enhancement of EM fields. More clearly, the field levels for high-frequency currents (i.e., beyond 100 MHz) decrease due to the presence of a metallic ground, and thereby, improving the SE of the bushing for these EM fields. The enhancement pattern for the axial E-fields is similar to the H-fields beyond the transition frequency.

The enhancement of EM field levels above the grounded protrusions in an actual substation has been calculated by considering a metallic structure of 550 mm (h) $\times$ 500 mm (w). This structure is placed on the ground plane at a radial distance of 2 m from the bushing. In the absence of metallic structure, the equipotential lines are uniform and parallel. Near the metallic structure, the equipotential lines may distort and become compressed. The compression results in increased amplitude of the transient fields in the computational cells that are close to the metallic structure. The increase in transient EM field amplitude is characterized in terms of the enhancement factor (EF). The transient EM field emission levels from the bushing are calculated, with and without the metallic structure, for a derivative Gaussian current excitation. From the study, it was understood that the EM field variation with time is oscillatory due to the metallic structure on the ground. At the same time, there is a remarkable change in the amplitude of the EM fields in the presence of the metallic structure. In order to understand the variation in enhancement of the field levels with frequency, EM fields have been calculated at just one cell above the metallic structure (see Fig. 10). The following observations have been made.

1) The field enhancement may not be linear with frequency and the same is dominant at limited frequencies only.
2) The enhancement factor for the radial E-fields is more compared to that of the axial E-fields and the H-fields. The EF for radial E-fields is dominant at corners of the structure.

Since the EF is a function of the observation point, the range of enhancement factors for EM fields at different frequencies is evaluated, by varying the physical location of the metallic structure (at different radial distances, e.g., from 0.5 to 4.0 m). The results are listed in Table III. The probability of occurrence of the EF above 20 for the radial E-fields and above 6 for the axial

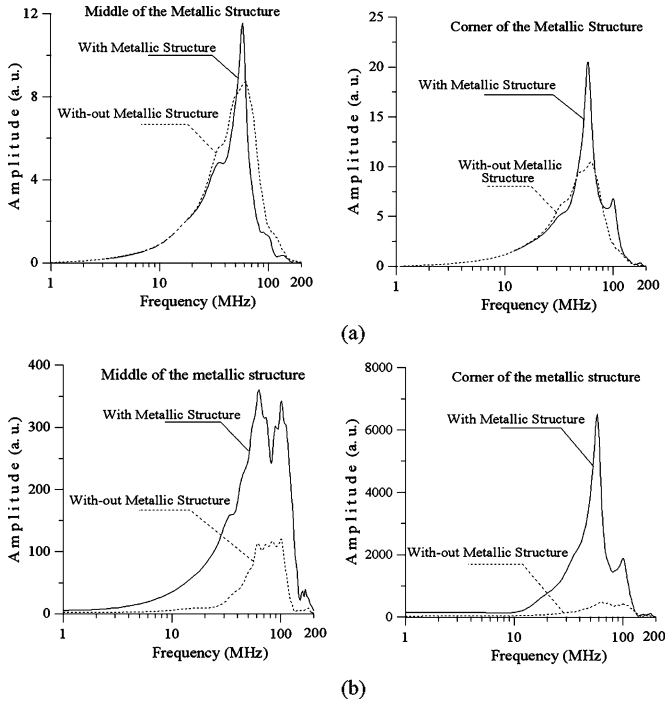

Fig. 10. Frequency spectra of the transient EM fields with a metallic structure on the ground plane. (a) H-field. (b) E_r-field.

E-fields is very low. The H-field enhancement is found to be highly dependent on the radial distance of the structure installation and is on the higher side, beyond the cut-off frequency. The radial E-field enhancement is more below the cut-off frequency. It is also understood that there is a low-field region at the middle of the metallic structure for the radial E-fields. This may be due to the fact that the tangential E-field just above the metallic structure is close to zero. The enhancement for axial E-fields is possible both at the middle and at the corners of the metallic structure. The change in the EF with the decrease in width of the metallic structure is found to be marginal. It has been further observed that the EF for EM fields with an insulating structure is very low compared to the EF with a metallic structure. This is true for the entire frequency range of the transient fields. More clearly, the EF for the transient EM fields changes considerably, depending on the existence of the metallic structure, insulated components, control wiring, and other phases of the GIS modules in the substation.

VIII. Transient EM Fields Due to VFTC

To quantify the emission levels in actual substation, the EM fields leaking out from the bushing have been evaluated for the VFTC waveform obtained during a switching event in the 245-kV GIS (shown in Fig. 1). Fig. 11 shows the transient EM fields at a radial distance of 2 m from the bushing, both in time and frequency scale. Here, the EM fields have been computed by assuming that the bushing was installed on a metallic sheet, with the support of an insulating kiosk/structure (3 m $\times$ 3 m, $\varepsilon_r = 3$), placed on a ground plane of conductivity 10^{-2} mho/m [see Fig 12(b)]. A metallic wall is also located at a radial distance

TABLE III
ENHANCEMENT FACTOR FOR THE TRANSIENT FIELDS DUE TO THE PRESENCE OF A METALLIC STRUCTURE ON THE GROUND PLANE

f (MHz)	Enhancement Factor (EF)		
	H_ϕ-Field	E_r–Field	E_z–Field
5	1.0-1.05	1.56-8.69	2.42-6.44
10	1.0-1.05	1.49-3.92	2.32-2.83
20	1.0-1.08	4.1-10.4	2.45-2.83
40	1.0-1.15	10.5-17.3	2.54-3.10
50	1.0-1.61	5.38-26.2	2.49-3.87
100	1.0-3.14	1.73-4.56	1.42-5.20
150	1.61-5.71	1.85-5.84	1.72-4.41
200	1.0-4.76	1.43-3.88	1.0-2.94

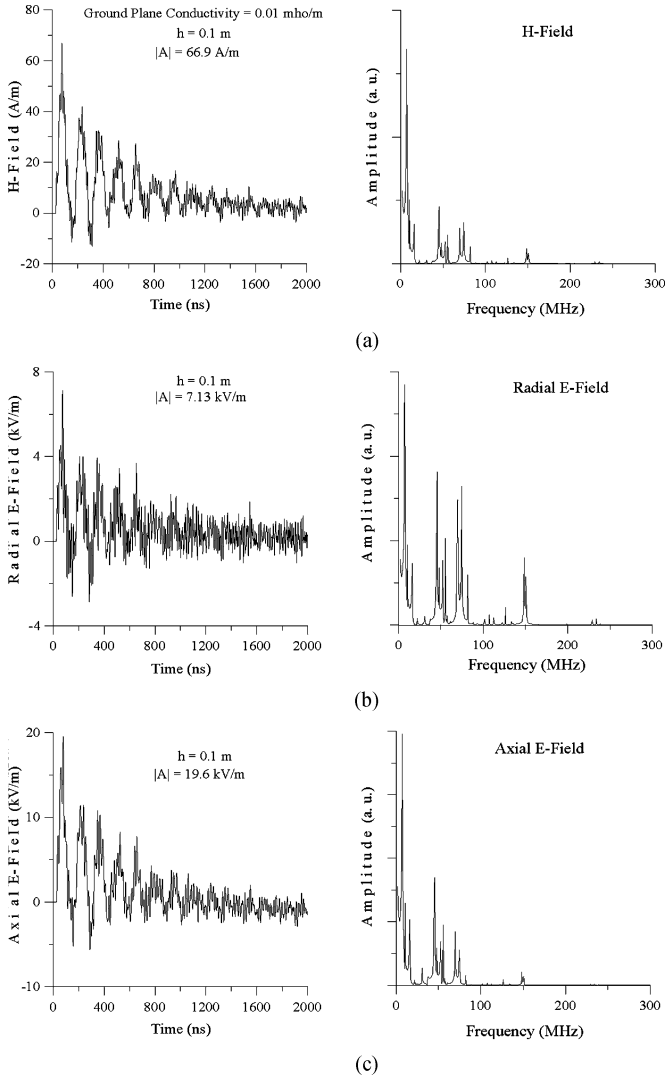

Fig. 11. Transient EM fields at a distance of 2 m from gas-to-air bushing.

of 4 m from the bushing, parallel to the kiosk, to simulate the actual GIS. The time-varying E-field waveforms attenuate to zero unlike in conventional substations, where they are proportional to the integration of the transient current [3], [4]. The dominant frequencies of the EM fields are almost in the same order as that for the VFTC waveform. However, the relative amplitudes of the dominant frequencies change in a considerable manner. From the analysis, it is evident that the EM fields are associated with high-frequency components up to 150 MHz as the

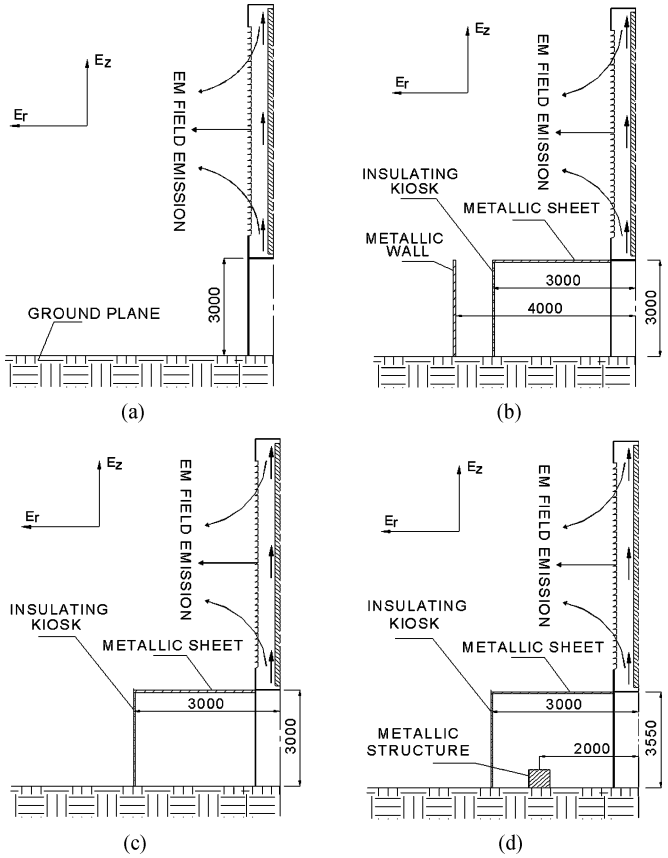

Fig. 12. Different bushing models under study. (a) Model I. (b) Model II. (c) Model III. (d) Model IV.

observation point is close to the ground (i.e., h = 0.1 m). This may be due to the multiple reflections among the metallic walls, insulating structure, and nearby ground. In order to understand the effect of the bushing installation on the emission levels in GIS, EM fields have been computed for the following models (see Fig. 12).

1) *Model I*: Bushing is installed at a height of 3 m from the ground.
2) *Model II*: Bushing is installed on a metallic sheet, with the support of an insulating kiosk. A metallic wall is kept at a radial distance of 4 m from bushing, parallel to the kiosk.
3) *Model III*: Bushing is installed on a metallic sheet, with the support of an insulating kiosk, placed on the ground plane.
4) *Model IV*: Bushing is installed on a metallic sheet, with the support of an insulating kiosk, placed on the ground plane. A metallic structure is kept on the ground.

As the observation point is close to the metallic wall, the transient E-field, which is tangential to the metallic wall, is considerably low (see Models I and II in Table IV). It is seen that the radial E-field levels increase with the increasing height above the ground. However, the H-field levels may not change to the considerable extent. This may be due to significant modification of the E-field pattern above the conductive ground. At the same time, the field levels decrease with the increasing distance from the bushing, and radial E-field levels tend to be low near the conductive ground. Radial and axial E-field levels computed at

TABLE IV
EM FIELD EMISSION LEVELS FOR VARIOUS BUSHING INSTALLATIONS

Model	Observation Point	H-Field (A/m)	E_r-Field (kV/m)	E_z-Field (kV/m)
Model-I	R = 1.0 m, h = 0.1 m	203.5	30.4	34.4
	R = 2.0 m, h = 0.1 m	104.6	9.7	38.8
	R = 2.0 m, h = 1.0 m	99.8	29.4	37.0
	R = 2.0 m, h = 2.0 m	99.4	85.5	46.7
Model – II	R = 1.0 m, h = 0.1 m	120.3	16.2	34.3
	R = 2.0 m ,h = 0.1 m	66.9	7.13	19.6
	R = 3.0 m, h = 0.1 m	42.9	2.22	9.05
	R = 2.0m , h = 0.5 m	63.9	11.5	18.8
	R = 2.0 m, h = 2.0 m	65.6	14.5	27.7
Model – III	R = 1.0 m, h = 0. 1m	121.5	16.5	32.2
	R = 2.0 m, h = 0.1 m	60.2	5.54	18.5
	R = 2.0 m, h = 1.0 m	58.7	12.3	18.6
	R = 2.0 m, h = 2.0 m	62.1	14.9	26.7
Model – IV (h is height above the structure)	R = 1.0 m, h = 0.1m	118.3	26.4	19.7
	R = 2.0 m, h = 0.1 m	55.8	22.0	46.2
	R = 2.0 m, h = 1.0 m	58.6	11.4	18.8
	R = 2.0 m, h = 2.0 m	60.4	19.2	26.7

a radial distance of 2 m and just above the ground are 7.13 and 19.6 kV/m, respectively (see Fig. 11, Model II in Table IV). The radial and axial E-field levels computed with a metallic structure on the ground at a radial distance of 2 m from the bushing are found to have considerable enhancement. These field levels are 22 and 53.4 kV/m, respectively. The average E-field enhancement factor is about 2 to 4 depending on the observation point for a particular VFTC. The H-field enhancement is found to be well below a factor of 2. This may be due to the fact that the EF for H-field is more beyond the cut-off frequency. However, the H-field waveform is dominant up to 74.5 MHz only. From the analysis, it is seen that the field levels reduce considerably due to the presence of conductive ground and the metallic walls/structures in the substation. More clearly, the complex substation equipment attenuate the EM fields with the increasing distance from the bushing, even though local enhancement is possible for these fields near the grounded protrusions.

IX. CONCLUSION

The transient EM field emission levels from the gas-to-air bushing through the composite insulator housing have been computed for the VFTCs generated during a switching event, using a numerical model based on the FDTD technique. The SE of the bushing for the EM fields is evaluated using a derivative Gaussian current source and a sinusoidal current source. The SE for H-fields decreases with the increase of frequency, and bushing does not offer any attenuation for the transient H-fields beyond the cut-off frequency. The SE pattern for the H-fields and the axial E-fields is almost similar beyond the transition frequency. The enhancement in the EM fields due to the presence of a metallic structure, which simulates the control cubicle or other phases of the grounded enclosures, was studied. The average enhancement factor is of the order of 2 to 4 for the E-fields and is well below 2 for the H-fields. The effect of conductivity of the ground plane on the EM field levels is found to be significant near the ground and is not considerable, as the observation point is a few meters away from the ground plane.

ACKNOWLEDGMENT

The authors would like to thank the management of Bharat Heavy Electricals Limited and the Indian Institute of Science for their permission to publish this work. Dr. Rao would like to thank Dr. H. S. Jain for his continuous encouragement and cooperation.

REFERENCES

[1] J. Meppelink, K. Diederich, K. Feser, and P. Pfaff, "Very fast transients in GIS," *IEEE Trans. Power Del.*, vol. 4, no. 1, pp. 223–233, Jan. 1989.
[2] D. E. Thomas, C. M. Wiggins, T. M. Salas, F. S. Nickel, and S. E. Wright, "Induced transients in substation cables: Measurements and models," *IEEE Trans. Power Del.*, vol. 9, no. 4, pp. 1861–1868, Oct. 1994.
[3] C. M. Wiggins and S. E. Wright, "Switching transient fields in substations," *IEEE Trans. Power Del.*, vol. 6, no. 2, pp. 591–600, Apr. 1991.
[4] C. M. Wiggins, D. E. Thomas, F. S. Nickel, T. M. Salas, and S. E. Wright, "Transient electromagnetic interference in substations," *IEEE Trans. Power Del.*, vol. 9, no. 4, pp. 1869–1884, Oct. 1994.
[5] S. Nishiwaki, K. Nojima, S. Tatara, M. Kosakada, N. Tanabe, and S. Yanabu, "Electromagnetic interference with electronic apparatus by switching surges in GIS-Cable system," *IEEE Trans. Power Del.*, vol. 10, no. 2, pp. 739–746, Apr. 1995.
[6] M. M. Rao, M. J. Thomas, and B. P. Singh, "Frequency characteristics of very fast transient currents (VFTC) in a 245 kV GIS," *IEEE Trans. Power Del.*, vol. 20, no. 4, pp. 2450–2457, Oct. 2005.
[7] K. S. Yee, "Numerical solution of initial boundary value problems involving Maxwell's equations in isotropic media," *IEEE Trans. Antennas Propag.*, vol. AP-101, no. 3, pp. 302–307, May 1966.
[8] G. Mur, "Absorbing boundary conditions for the finite difference approximation of the time-domain electromagnetic field equations," *IEEE Trans. Electromagn. Compat.*, vol. EMC-23, no. 4, pp. 377–382, Nov. 1981.
[9] A. Taflove, K. R. Umashankar, B. Beker, F. Harfoush, and K. S. Yee, "Detailed FD-TD analysis of electromagnetic fields penetrating narrow slots and lapped joints in thick conducting screens," *IEEE Trans. Antennas Propag.*, vol. 36, no. 2, pp. 247–257, Feb. 1988.
[10] M. M. Rao, M. J. Thomas, and B. P. Singh, "Computation of EMI fields in a high voltage gas insulated substation during switching operations," in *Proc. IEEE Int. Symp. Electromagn. Compat.*, Boston, MA, Aug. 18–22, 2003, vol. 3, pp. 743–748.
[11] M. M. Rao, M. J. Thomas, B. P. Singh, and P. Rajagopalan, "Computation and measurement of electromagnetic interference generated during switching events in a GIS," CIGRE, Paris, 2004.

M. Mohana Rao was born in Guntur, Andhra Pradesh, India, in 1973. He received the B.Tech. degree in engineering from Sri Venkateswara University, Tirupathi, India, and the M.Sc. and Ph.D. degrees in engineering, from the Indian Institute of Science, Bangalore, in 1994, 1996, and 2006, respectively.

Currently, he is a Deputy Manager with Bharat Heavy Electricals Limited, Corporate R&D, Hyderabad, India. His current research interests include design and development of gas-insulated substations (GIS), gas-insulated lines, surge arresters, electromagnetic interference/electromagnetic compatibility studies in GIS, digital signal processing techniques in power systems, and computational fluid dynamics-based analysis of circuit breaker arcs.

M. Joy Thomas was born in Kerala, India, in 1961. He received the B.Tech. degree in electrical engineering from the Institute of Technology, Benaras Hindu University, India, and the M.Sc. and Ph.D. degrees in engineering from the Indian Institute of Science, Bangalore, in 1983, 1986, and 1993, respectively.

He is currently an Assistant Professor in the Department of High Voltage Engineering, Indian Institute of Science.

His current research interests include gas-insulated switchgear, electromagnetic interference/electromagnetic compatibility, high-power electromagnetics, digital measurement of high voltages and currents, pulsed power engineering, extra high voltage (HV) power transmission, electrical transients in power systems, condition monitoring of HV power apparatus, nano dielectrics, and insulation engineering.

B. P. Singh was born in Bihar, India, in 1947. He received the B.E. degree from the Muzaffarpur Institute of Technology, India, the M.E. degree from the Indian Institute of Science, Bangalore, and the Ph.D. degree from the University of Liverpool, Liverpool, U.K., in 1968, 1971, and 1974, respectively, all in electrical engineering.

He was a Postdoctoral Fellow with the University of Liverpool in a project sponsored by the U.K. Atomic Energy agency for a year. Then, he worked with the Reactor Research Centre, Kalpakkam, India, for two years. Currently, he is a General Manager with Bharat Heavy Electricals Limited, Corporate R&D, Hyderabad, India. His current research interests include switchgear, power transformers, motors, and capacitors. He has published about 100 research papers in various national and international journals and conference proceedings.